J|A|C|S ARTICLES

Published on Web 05/26/2009

Consequences of Conformational Preorganization in Sesquiterpene Biosynthesis: Theoretical Studies on the Formation of the Bisabolene, Curcumene, Acoradiene, Zizaene, Cedrene, Duprezianene, and Sesquithuriferol Sesquiterpenes

Young J. Hong and Dean J. Tantillo*

Department of Chemistry, University of California, Davis, One Shields Avenue, Davis, California 95616

Received January 22, 2009; E-mail: tantillo@chem.ucdavis.edu

Abstract: Quantum chemical calculations on cyclization mechanisms for several sesquiterpene families proposed to be closely related to each other in a biogenic sense (the bisabolene, curcumene, acoradiene, zizaene (zizaene, isozizaene, *epi*-zizaene, and *epi*-isozizaene), cedrene (α/β-cedrenes and 7-*epi*-α/β-cedrenes), duprezianene, and sesquithuriferol families) are described. On the basis of the results of these calculations, we suggest that the conformation of the bisabolyl cation attainable in an enzyme active site is a primary determinant of the structure and relative stereochemistry of the sesquiterpenes formed. We also suggest that substantial conformational changes of initially formed conformers of the bisabolyl cation are necessary in order to form zizaene and *epi*-cedrene. Given that the productive conformation of the bisabolyl cation does not necessarily reflect the original orientation of farnesyl diphosphate bound in the corresponding enzyme active site, we conclude that folding of farnesyl diphosphate alone does not always dictate the structure and relative stereochemistry of cyclization products. In addition, the potential roles of dynamic matching in determining product distributions and enzyme-promoted formation of secondary carbocations are discussed.

1. Introduction

In Nature, most sesquiterpenes are formed from complex rearrangement reactions of carbocations derived from farnesyl diphosphate (FPP). These reactions occur under the control of a class of enzymes known as the sesquiterpene synthases (or cyclases).[1−6] The diverse array of structurally and stereochemically complex organic molecules derived from the simple acyclic and achiral FPP has fascinated organic chemists and biochemists for decades. Many elegant studies on the enzymes responsible for these remarkable transformations have provided important insights into the mechanisms of the rearrangement reactions.[1–6] In general, the proposed reaction mechanisms for sesquiterpene formation consist of three major stages: (1) generation of a carbocation, (2) carbocationic rearrangements, and (3) neutralization of a carbocation, either by deprotonation or capture of a nucleophile (e.g., water).[2] It is our goal to use modern computational quantum chemistry to provide additional insights into the second stage of sesquiterpene-forming reactions, i.e. to provide detailed pictures of the intermediates and transition-state structures involved in the carbocation rearrangements that lead to complex sesquiterpenes.[7−11]

The sesquiterpene synthase enzymes mediate the transformation of relatively simple carbocations into much more complex structures. For example, Scheme 1 depicts some of the routes that have been proposed to connect the bisabolyl cation (blue), a relatively simple carbocation intermediate produced by one mode of cyclization (1,6-closure after isomerization of FPP; red), to a diverse array of complex natural products.[2,12−17] Hundreds of other sesquiterpene products are thought to arise via different cyclization modes. In general, a given synthase enzyme produces one or a few specific natural products in high yield out of this broad array of possibilities, although several more promiscuous synthases have been described.[18−20]

(1) Cane, D. E. *Sesquiterpene biosynthesis: cyclization mechanisms*; Elsevier: The Netherlands, 1999; Vol. 2, pp 155−200.
(2) Cane, D. E. *Chem. Rev.* **1990**, *90*, 1089–1103.
(3) Cane, D. E. *Acc. Chem. Res.* **1985**, *18*, 220–226.
(4) Christianson, D. W. *Chem. Rev.* **2006**, *106*, 3412–3442.
(5) Davis, E. M.; Croteau, R. *Top. Curr. Chem.* **2000**, *209*, 53–95.
(6) Christianson, D. W. *Curr. Opin. Chem. Biol.* **2008**, *12*, 141–150.
(7) Lodewyk, M. W.; Gutta, P. G.; Tantillo, D. J. *J. Org. Chem.* **2008**, *73*, 6570–6579.
(8) Ho, G. A.; Nouri, D. H.; Tantillo, D. J. *J. Org. Chem.* **2005**, *70*, 5139–5143.
(9) Gutta, P.; Tantillo, D. J. *J. Am. Chem. Soc.* **2006**, *128*, 6172–6179.
(10) Hong, Y. J.; Tantillo, D. J. *Org. Lett.* **2006**, *8*, 4601–4604.
(11) Wang, S. C.; Tantillo, D. J. *Org. Lett.* **2008**, *10*, 4827–4830.
(12) Dewick, P. M. *Nat. Prod. Rep.* **2002**, *19*, 181–222.
(13) Parker, W.; Roberts, J. S.; Ramage, R. *Q. Rev. Chem. Soc.* **1967**, *21*, 331–363.
(14) Cool, L. G. *Phytochemistry* **2005**, *66*, 249–260.
(15) Jones, C. G.; Ghisalberti, E. L.; Plummer, J. A.; Barbour, E. L. *Phytochemistry* **2006**, *67*, 2463–2468.
(16) Mercke, P.; Crock, J.; Croteau, R.; Brodelius, P. E. *Arch. Biochem. Biophys.* **1999**, *369*, 213–222.
(17) Wu, S.; Schoenbeck, M. A.; Greenhagen, B. T.; Takahashi, S.; Lee, S.; Coates, R. M.; Chappell, J. *Plant. Physiol.* **2005**, *138*, 1322–1333.

Scheme 1

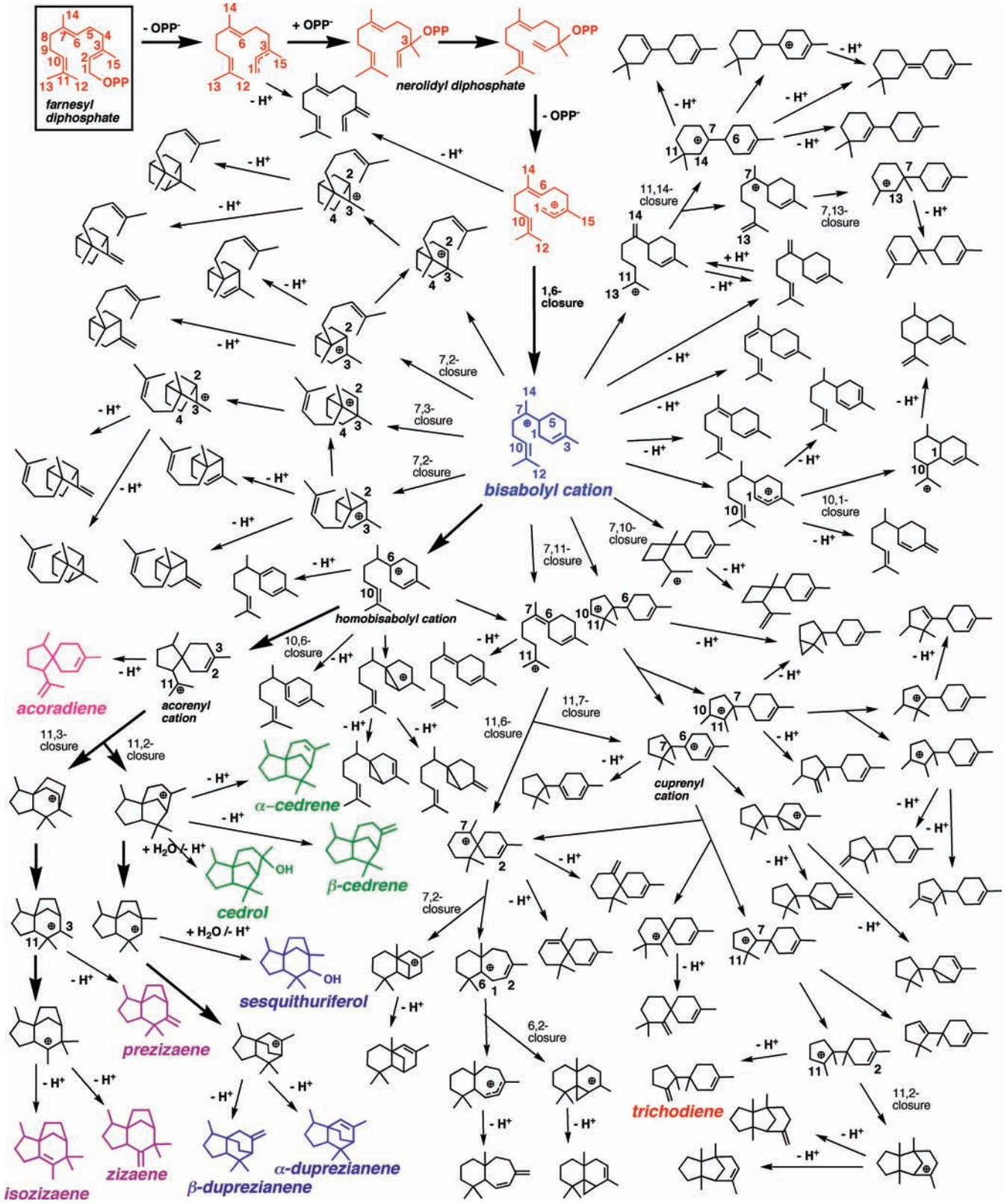

Recently, several publications on manipulating the structure of sesquiterpene synthases by mutation of residues within or surrounding the active site have suggested that a few key structural elements (plasticity residues) are critical in controlling the selectivity of product formation.[19,21−23] The wide variety of changes in product distributions observed upon mutation of synthase enzymes reflects a range of shifts in mechanism from subtle to dramatic.[19,21–30] Still, the atomic-level details of how changes in the structure of synthases lead to changes in product

(18) Little, D. B.; Croteau, R. B. *Arch. Biochem. Biophys.* **2002**, *402*, 1201–1235.

Chart 1. Structures of Zizaene, Cedrene, Acoradiene, Dueprezianene and Sesquithuriferol Sesquiterpenes: (7*S*)-Isozizaene = *epi*-Isozizaene (**1**),[33] (7*S*,10*R*)-Zizaene = *epi*-zizaene (**2**), (7*R*)-Isozizane = Isozizaene (**3**), (7*R*,10*R*)-Zizaene = Zizaene (**4**),[41] (7*S*,10*S*)-Zizaene (**5**), (7*R*,10*S*)-Zizaene (**6**), (7*S*,10*S*)-Prezizaene (**7**), (7*R*,10*S*)-Prezizaene (**8**),[41] (7*S*,10*R*)-Prezizane (**9**),[39] (7*R*,10*R*)-Prezizaene (**10**), (7*S*,10*S*)-Acoradiene = β-Acoradiene (**11**), (7*R*,10*S*)-Acoradiene = *epi*-β-Acoradiene (**12**), (7*S*,10*R*)-Acoradiene = α-Acoradiene (**13**),[16,39] (7*R*,10*R*)-Acoradiene = *epi*-α-Acoradiene (**14**), (7*S*,10*R*)-α-Cedrene = α-Cedrene (**15**),[39] (7*S*,10*R*)-β-Cedrene = β-Cedrene (**16**), (7*R*,10*R*)-α-Cedrene = *epi*-α-Cedrene (**17**), (7*R*)-β-Cedrene = *epi*-β-Cedrene (**18**), (7*S*,10*S*)-α-Cedrene (**19**), (7*S*,10*S*)-β-Cedrene (**20**), (7*R*,10*S*)-α-Cedrene (**21**), (7*R*,10*S*)-β-Cedrene (**22**),[37] (3*R*,7*S*,10*R*)-Cedrol = *epi*-Cedrol (**23**),[16] (3*S*,7*S*,10*R*)-Cedrol = Cedrol (**24**), (3*R*,7*R*,10*R*)-Cedrol (**25**), (3*S*,7*R*,10*R*)-Cedrol (**26**), (3*R*,7*S*,10*S*)-Cedrol (**27**), (3*S*,7*S*,10*S*)-Cedrol (**28**), (3*R*,7*R*,10*S*)-Cedrol (**29**), (3*S*,7*R*,10*S*)-Cedrol (**30**), (2*S*,7*S*,10*R*)-Sesquithuriferol (**31**),[42] (2*R*,7*S*,10*R*)-Sesquithuriferol (**32**), (2*S*,7*R*,10*R*)-Sesquithuriferol (**33**),[38] (2*R*,7*R*,10*R*)-Sesquithuriferol (**34**),[43] (7*S*,10*S*)-α-Duprezianene (**35**), (2*S*,7*S*,10*S*)-β-Duprezianene (**36**), (2*S*,7*R*,10*S*)-α-Duprezianene (**37**),[38,44] (2*S*,7*R*,10*S*)-β-Duprezianene (**38**)[38,44*a*]

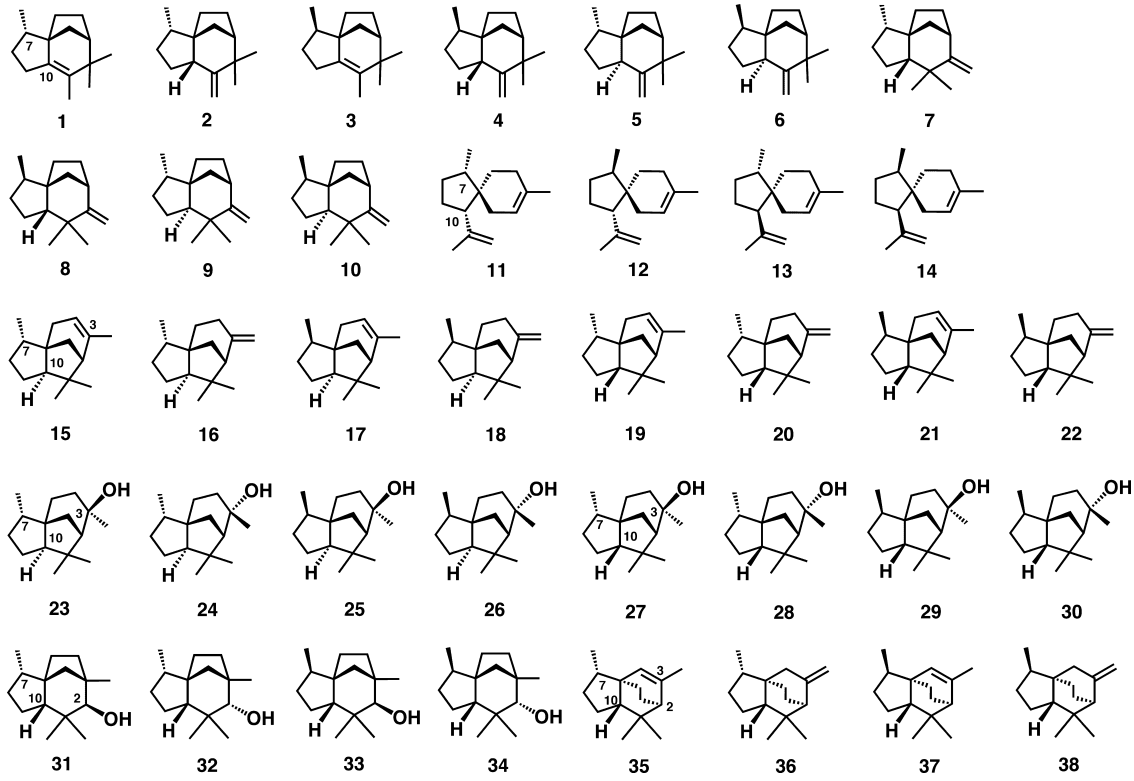

[a] Atom numbers shown correspond to the standard numbering for FPP (Scheme 1).

distributions remain, in large part, unclear. Such details are relevant to both the natural process of divergent functional evolution of these enzymes and the design of mutagenesis experiments, perhaps for the rational creation of sesquiterpene synthases with altered product distributions.[31]

To investigate the connections between carbocation rearrangement mechanisms and structural divergence from bisabolyl-type intermediates, we chose several sesquiterpene families proposed to have closely related biogenic origins:[13] the bisabolene,[32] curcumene,[13,29] acoradiene,[16,33] zizaene (zizaene,[34] isozizaene, *epi*-zizaene and *epi*-isozizaene[33]), cedrene (α/β-

(19) Yoshikuni, Y.; Ferrin, T. E.; Keasling, J. D. *Nature* **2006**, *440*, 1078–1082.
(20) Köllner, T. G.; O'Maille, P. E.; Gatto, N.; Boland, W.; Gershenzon, J.; Degenhardt, J. *Arch. Biochem. Biophys.* **2006**, *448*, 83–92.
(21) Greenhagen, B. T.; O'Maille, P. E.; Noel, J. P.; Chappell, J. *Proc. Natl. Acad. Sci. U.S.A.* **2006**, *103*, 9826–9831.
(22) Vedula, L. S.; Rynkiewicz, M. J.; Pyun, H. J.; Coates, R. M.; Cane, D. E.; Christianson, D. W. *Biochemistry* **2005**, *44*, 6153–6163.
(23) Vedula, L. S.; Cane, D. E.; Christianson, D. W. *Biochemistry* **2005**, *44*, 12719–12727.
(24) Cane, D. E.; Xue, Q. *J. Am. Chem. Soc.* **1996**, *118*, 1563–1564.
(25) Whittington, D. A.; Wise, M. L.; Urbansky, M.; Coates, R. M.; Croteau, R. B.; Christianson, D. W. *Proc. Natl. Acad. Sci. U.S.A.* **2002**, *99*, 15375–15380.
(26) Cane, D. E.; Xue, Q.; Fitzsimons, B. C. *Biochemistry* **1996**, *35*, 12369–12376.
(27) Back, K.; Chappell, J. *Proc. Natl. Acad. Sci. U.S.A.* **1996**, *93*, 6841–6845.
(28) Hyatt, D. C.; Croteau, R. *Arch. Biochem. Biophys.* **2005**, *439*, 222–233.
(29) Köllner, T. G.; Schnee, C.; Gershenzon, J.; Degenhardt, J. *Plant Cell* **2004**, *16*, 1115–1131.
(30) Lodeiro, S.; Segura, M. J.; Stahl, M.; Schulz-Gasch, T.; Matsuda, S. P. *ChemBioChem.* **2004**, *5*, 1581–1585.
(31) Chappell, J. *Curr. Opin. Plant Biol.* **2002**, *5*, 151–157.
(32) Ruzicka, L. *Pure Appl. Chem.* **1963**, *6*, 493–523.
(33) Lin, X.; Hopson, R.; Cane, D. E. *J. Am. Chem. Soc.* **2006**, *128*, 6022−6023. In this paper, the authors reported that *epi*-isozizaene produced by the recombinant synthase cloned from *Streptomyces coelcolor* is enantiomeric to the known synthetic (−)-*epi*-isozizaene prepared by formic acid-catalyzed rearrangement of (+)-zizaene (see ref 41). Note also that while our manuscript was under review, Lin and Cane reported additional mechanistic experiments on *epi*-isozizaene synthase (Lin, X.; Cane, D. E. *J. Am. Chem. Soc.* **2009**, *131*, 6332–6333). Using labeling experiments, these authors demonstrated that C12, rather than C13, methyl group migration occurs, consistent with our predicted inherent preference for C12 methyl migration. In addition, several of the other sesquiterpenes described herein were identified as minor products of *epi*-isozizaene synthase.
(34) Pati, L. C.; Roy, A.; Mukherjee, D. *Tetrahedron* **2002**, *58*, 1773–1778.

Scheme 2

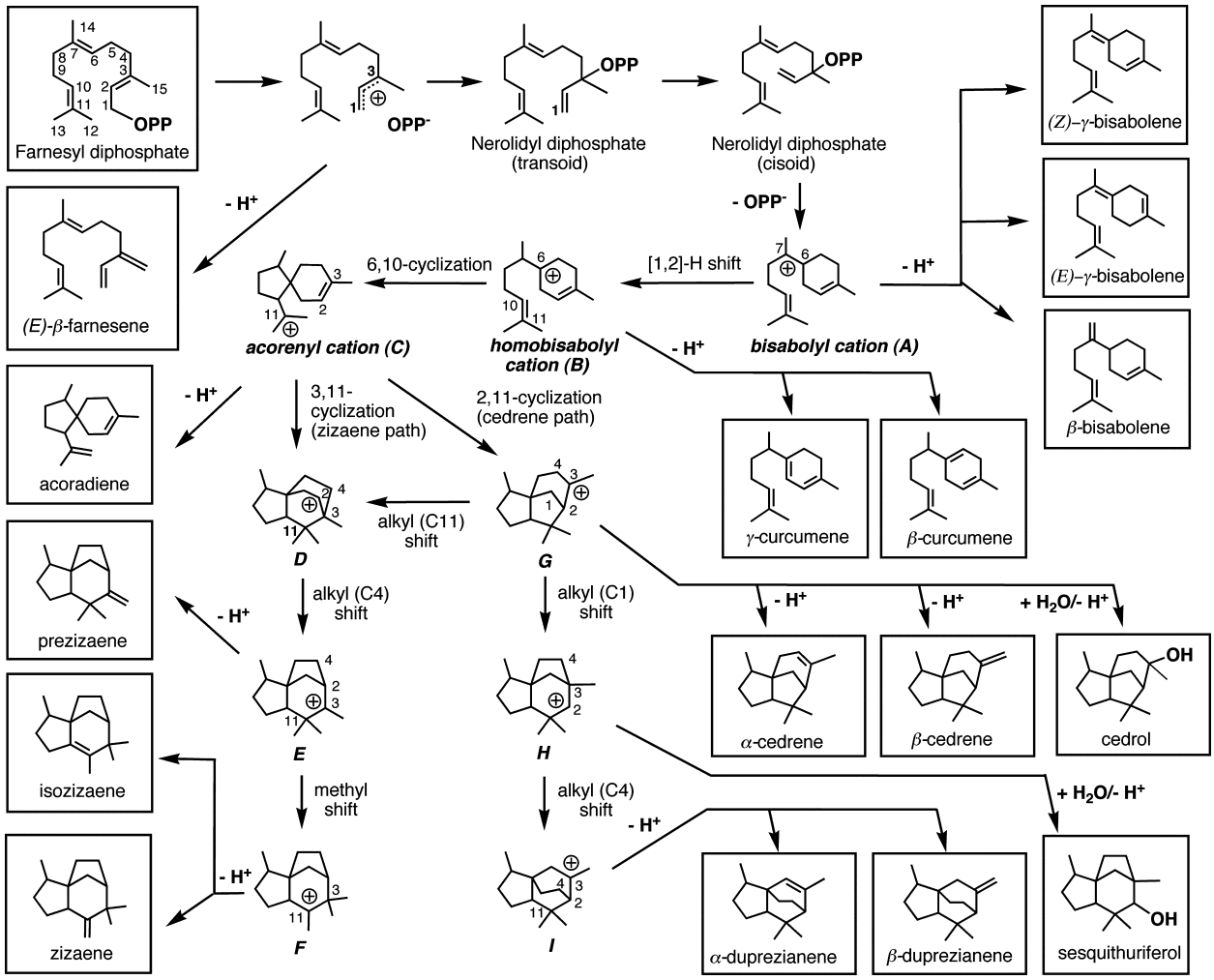

cedrenes and 7-*epi*-α/β-cedrenes),[16,35−37] duprezianene,[37,38] and sesquithuriferol[37,38] families (Scheme 1, blue, and Chart 1). Typical mechanisms proposed for the production of these sesquiterpenes are shown in Scheme 2.[16,33,39] For simplicity, this scheme shows the formation of the hydrocarbon skeletons without explicit stereochemistry (*vide infra*). The common reaction pathway leading to all of these sesquiterpenes involves three carbocationic intermediates: the bisabolyl cation, the homobisabolyl cation, and the acorenyl cation (Scheme 2). From the acorenyl cation, the pathway branches to the cedrene pathway (2,11-cyclization) and the zizaene pathway (3,11-cyclization).[40]

Herein we describe detailed mechanisms for the formation of the structures shown in Chart 1.[45] These mechanisms are based on the results of quantum chemical calculations. Our results allow us to propose plausible and testable explanations for the origins of the different sesquiterpene skeletons of these natural products, as well as a potentially general model for how the evolution of sesquiterpene synthases can lead to high selectivity for particular products.

2. Methods

All calculations were performed with GAUSSIAN03.[46] All geometries were optimized using the B3LYP/6-31+G(d,p) method.[47−50] All stationary points were characterized by frequency calculations and reported energies include zero-point energy cor-

(35) Although no previous report, to our knowledge, has ever suggested the possibility of the rearrangement of (7*R*,10*R*)-cedrene (*epi*-cedrene) (**17** or **18**) to (7*R*)-isozizaene (**3**), the rearrangement of (7*S*,10*R*)-cedrene (**15** or **16**) to *epi*-isozizaene (**1**) in superacid has been observed. See Polovinkaa, M. P.; Korchaginaa, D. V.; Shcherbukhin, V. V.; Gatilova, Y. V.; Rybalovaa, Y. V.; Zefirovb, N. S.; Barkhash, V. A. *Tetrahedron Lett.* **1995**, *36*, 8093–8096.

(36) Kreipl, A. T.; König, W. A. *Phytochemistry* **2004**, *65*, 2045–2049.

(37) Barrero, A. F.; Quilez Del Moral, J.; Lara, A. *Tetrahedron* **2000**, *56*, 3717–3723.

(38) Barrero, A. F.; Alvarez-Manzaneda, E.; Lara, A. *Tetrahedron Lett.* **1996**, *37*, 3757–3760.

(39) O'Maille, P. E.; Chappell, J.; Noel, J. P. *Arch. Biochem. Biophys.* **2006**, *448*, 73–82.

(40) The reaction mechanism shown for zizaene is based on that described in a recent report (see reference 33) on the isolation of *epi*-isozizaene from the reaction catalyzed by a recombinant synthase cloned from *Streptomyces coelcolor*, and the mechanism shown for the cedrenes is based on that proposed in another recent report (see reference 16) on recombinant *epi*-cedrol synthase, cloned from *Artemissia annua L.*

(41) Andersen, N. H.; Smith, S. E.; Ohta, Y. J. C. S. *Chem. Commun.* **1973**, 447–448.

(42) Fukushi, Y.; Yajima, C.; Mizutani, J. *Tetrahedron Lett.* **1994**, *35*, 8809–8812.

(43) Carrol, P. J.; Ghisalberti, E. L.; Ralph, D. E. *Phytochemistry* **1976**, *15*, 777–780.

(44) Piovetti, L.; Diara, A. *Phytochemistry* **1977**, *16*, 103–106.

(45) This report is part 5 in our "Theoretical Studies on Farnesyl Cation Cyclization" series. For parts 1−4 and leading references to related work, see refs 7 and 9−11.

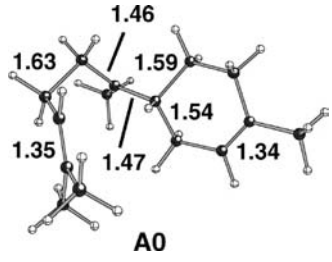

Figure 1. Structure of (*R*)-bisabolyl cation conformer (**A0**) whose energy was set to [0.00] kcal/mol for all energy comparisons.

rections (unscaled). Intrinsic reaction coordinate (IRC) calculations were used for further characterization of all transition state structures.[51,52] The B3LYP method is known to perform reasonably well in the prediction of geometries and behavior of carbocations.[7–11,53–56] A recent report on density functional theory (DFT) methods also shows that B3LYP performs well in describing overall physical properties for biologically relevant small molecules in biological systems such as proteins, DNA, and RNA, in particular with large Pople-type basis sets.[57] To address the purported systematic tendency of the B3LYP method to underestimate reaction energies of hydrocarbon *cyclization* reactions, which was described in a recent report by Matsuda and co-workers, we include single point energies using a different functional, mPW1PW91, that is reported to correct this problem (i.e., the mPW1PW91/6-31+G(d,p)//B3LYP/6-31+G(d,p) level), for comparison.[58] These energies include unscaled zero-point energy corrections from B3LYP/6-31+G(d,p) frequency calculations. We have used these methods previously in studies of other terpene-forming carbocation rearrangement reactions.[7–11,56] All energies for intermediate structures and transition-state structures in this report are expressed in kcal/mol and are relative to that of the bisabolyl cation conformer **A0** (Figure 1) whose energy is set to [0.00] kcal/mol. Structural drawings were produced using Ball & Stick.[59] Atom numbering indicated in the structures in this report refers to that of FPP (Scheme 1). Throughout the manuscript, numbers are used to label natural products and letters are used to label carbocations. Numbers following letters for carbocations are used to label different conformations.

3. Results and Discussion

Configuration and Conformations of the Bisabolyl Cation. The generally proposed mechanisms for the conversion of FPP to the sesquiterpenes of interest (Scheme 1) begin with isomerization of FPP to nerolidyl diphosphate (NPP), which then cyclizes (with the loss of pyrophosphate, either via ionization followed by cyclization or via direct displacement of the pyrophosphate group by the C6=C7 π-bond of nerolidyl diphosphate) to form a methylcyclohexene-substituted carbocation, the bisabolyl cation (Schemes 1−2).[3–5] In principle, this cation could be formed with either *R* or *S* absolute configuration. The computed structures shown below are all based on the (*R*)-bisabolyl cation to facilitate comparisons between them, although we do not know for certain what the true absolute configuration is in Nature for most cases.[1–44] This issue is addressed further near the end of our discussion.

In our previous study on trichodiene formation,[10] we encountered various productive conformers of the bisabolyl cation. During the current study, we uncovered additional relevant conformers. We chose to set the relative energy of bisabolyl conformer **A0** (Figure 1), the cation that was also utilized as a reference in our previous study, to [0.00] kcal/mol to facilitate comparisons between the many different sesquiterpene-forming pathways that involve bisabolyl cations.

Formation of *epi*-Isozizaene (1), (7*S*,10*R*)-Zizaene (2), (7*S*,10*S*)-Prezizaene (7) and (6*R*,7*S*,10*S*)-Acoradiene (11). In this section, we describe in detail the results of calculations on the pathway from one particular conformer of the bisabolyl cation to several sesquiterpene natural products. In subsequent sections on pathways to other sesquiterpenes we go into less detail and instead highlight just the unique features of these pathways. Details on all computed structures can be found in the Supporting Information.

A0 is a productive conformer for a hydride shift that occurs via the "interior" face of the acyclic chain of the bisabolyl cation.[60] However, this hydride shift imposes a conformational impediment on the subsequent 6,10-cyclization of the resultant homobisabolyl cation, the cyclization that would produce the acorenyl cation (Scheme 2). Therefore, we looked for a bisabolyl cation conformer that is productive in terms of both the [1,2]-hydride shift and the subsequent 6,10-cyclization. A complete reaction pathway from this conformer of the bisabolyl cation, **A1**, to *epi*-isozizaene (**1**) and (7*S*,10*R*)-zizaene (*epi*-zizaene, **2**), based on our calculations, is shown in Scheme 3 (right) and Figure 2. Note that only those conformers of a given carbocation (**A**−**F**) that are productive for a rearrangement reaction in the pathway leading to **1** and **2** and/or that result directly from a rearrangement reaction occurring in that pathway are shown. This pathway also leads to (7*S*,10*S*)-prezizaene (**7**), (6*R*,7*S*,10*S*)-acoradiene (β-acoradiene) (**11**), (6*E*)-γ-bisabolene, and α/β-bisabolene (Scheme 3).

The first step after the formation of the bisabolyl cation in the proposed mechanism (Schemes 2 and 3) is a [1,2]-hydride shift between carbons 6 and 7. Hydride shift via the "exterior" face of the acyclic chain of the bisabolyl cation is required to form a conformation productive for subsequent reactions. This hydride shift converts bisabolyl cation **A1** into cation **B1** (Scheme 3, right and Figure 2), one conformer of the homobisabolyl cation. The transition structure for this sigmatropic rearrangement resembles a nonclassical carbocation with a 3-center 2-electron [C···H···C] delocalized bonding array.[61−64] The barrier for conversion of **A1** to **B1** is calculated to be ~6−7 kcal/mol.

(46) Frisch, M. J.; et al. *Gaussian03*, revision D.01; Gaussian, Inc.: Pittsburgh, PA, 2003 (see full reference in Supporting Information).
(47) Becke, A. D. *J. Chem. Phys.* **1993**, *98*, 5648–5652.
(48) Becke, A. D. *J. Chem. Phys.* **1993**, *98*, 1372–1377.
(49) Lee, C.; Yang, W.; Parr, R. G. *Phys. Rev. B* **1988**, *37*, 785–789.
(50) Stephens, P. J.; Devlin, F. J.; Chabalowski, C. F.; Frisch, M. J. *J. Phys. Chem.* **1994**, *98*, 11623–11627.
(51) Gonzalez, C.; Schlegel, H. B. *J. Phys. Chem.* **1990**, *94*, 5523–5527.
(52) Fukui, K. *Acc. Chem. Res.* **1981**, *14*, 363–368.
(53) Hong, Y. J.; Tantillo, D. J. *J. Org. Chem.* **2007**, *72*, 8877–8881.
(54) Gutta, P.; Tantillo, D. J. *Angew. Chem., Int. Ed.* **2005**, *44*, 2719–2723.
(55) Bojin, M. D.; Tantillo, D. J. *J. Phys. Chem. A* **2006**, *110*, 4810–4816.
(56) Gutta, P.; Tantillo, D. J. *Org. Lett.* **2007**, *9*, 1069–1071.
(57) Riley, K. E.; Op't Holt, B. T.; Merz, K. M. *J. Chem. Theory Comput.* **2007**, *3*, 407–433.
(58) Matsuda, S. P. T.; Wilson, W. K.; Xiong, Q. *Org. Biomol. Chem.* **2006**, *4*, 530–543.
(59) Müller, N.; Falk, A.; Gsaller, G. *Ball & Stick*, V.4.0a12, molecular graphics application for MacOS computers; Johannes Kepler University: Linz, 2004.
(60) Hong, Y. J.; Tantillo, D. J. Unpublished results.
(61) Grob, C. A. *Acc. Chem. Res.* **1983**, *16*, 426–431.
(62) Brown, H. C. *Acc. Chem. Res.* **1983**, *16*, 432–440.
(63) Olah, G. A.; Prakash, G. K. S.; Saunders, M. *Acc. Chem. Res.* **1983**, *16*, 440–448.
(64) Walling, C. *Acc. Chem. Res.* **1983**, *16*, 448–454.

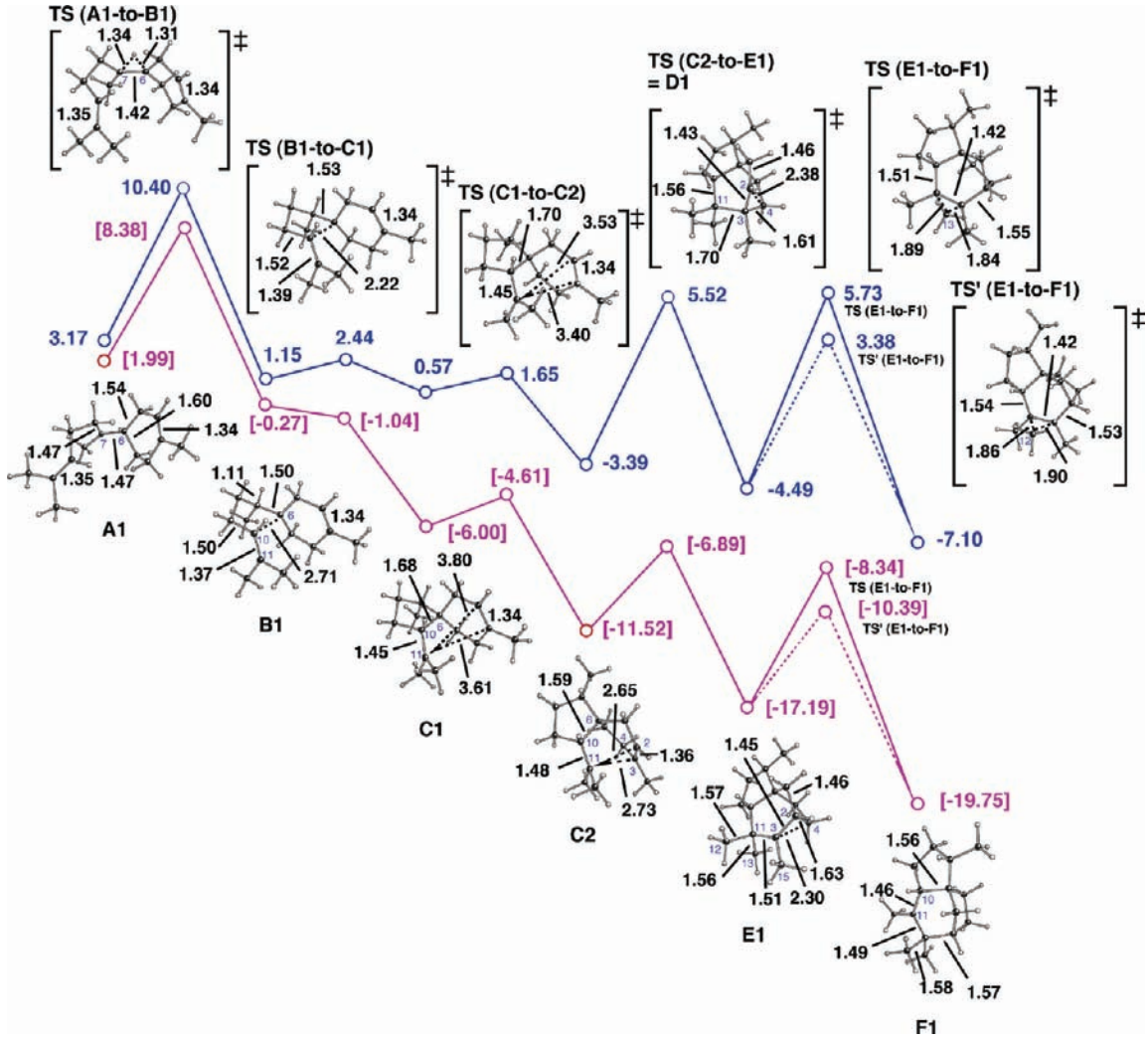

Figure 2. Conversion of bisabolyl cation conformer **A1** to **F1**, the cation that precedes *epi*-isozizaene (**1**) and (7*S*,10*R*)-zizaene (*epi*-zizaene) (**2**). Computed geometries (selected distances in Å) and relative energies (in kcal/mol) of intermediates and transition structures are shown. Blue pathway: B3LYP/6-31+G(d,p)//B3LYP/6-31+G(d,p). Plum pathway: mPW1PW91/6-31+G(d,p)//B3LYP/6-31+G(d,p).

Attack by the C10═C11 π-bond on the pro-*R* face of the C6 cationic center then directly converts **B1** to the acorenyl cation **C1**. The transition structure for this intramolecular cation-alkene addition reaction resembles **B1** in terms of both geometry and energy; note the relatively small difference between the C6−C10 distances in **B1** and the transition structure (~0.5 Å) and that there is essentially no energetic barrier. Direct deprotonation of **C1** would generate (6*R*,7*S*,10*S*)-acoradiene (*epi*-β-acoradiene) (**11**).

The next rearrangement step has been proposed to involve 3,11-cyclization, which would form a secondary cation (Scheme 2).[33] **C1** appears to be a nonproductive conformation with respect to 3,11-cyclization, however. We did find an alternative productive conformer of the acorenyl cation, **C2**, which is also thermodynamically favored by ~4−6 kcal/mol (Figure 2). In **C1**, there is strong hyperconjugation between the C6−C10 σ-bond (elongated to 1.68 Å) and cationic carbon C11, which shortens the C10−C11 bond to 1.45 Å. In conformer **C2**, the hyperconjugation between the C6−C10 σ-bond and cationic carbon C11 is diminished (note that the C6−C10 distance is shortened to 1.59 Å and the C10−C11 bond is elongated to 1.48 Å), however cationic carbon C11 interacts with the C2═C3 π-bond (which is slightly elongated to 1.36 Å). It appears that this intermolecular cation-π interaction[4,65,66] affords additional thermodynamic stability to **C2**. We also located a transition structure connecting **C1** to **C2** (Figure 2) via a computed barrier of only ~1−2 kcal/mol from **C1**.

3,11-Cyclization of **C2** would lead to the secondary cation **D** (Scheme 2),[33] but we were unable to locate a minimum corresponding to **D**. Instead we found a structure, **D1,** that resembles the expected secondary cation but is a transition structure connecting **C2** directly to **E1** (Scheme 3, right and Figure 2). This direct conversion of **C2** into cation **E1** differs from previously proposed mechanistic hypotheses. The barrier for this rearrangement is ~5−9 kcal/mol from **C2**. Generation of **E1** involves a concerted rearrangement reaction with two events that occur asynchronously: cyclization and alkyl shift (Figure 3).[67] In this process, two new σ-bonds (C3−C11 and C2−C4) are formed. The concerted reaction mechanism allows the system to avoid the formation of a discrete secondary cation intermediate, although, as mentioned above, the transition

(65) Dougherty, D. A. *Science* **1996**, *271*, 163–168.
(66) Jenson, C.; Jorgensen, W. L. *J. Am. Chem. Soc.* **1997**, *119*, 10846–10854.
(67) Tantillo, D. J. *J. Phys. Org. Chem.* **2008**, *21*, 561–570.

Scheme 3

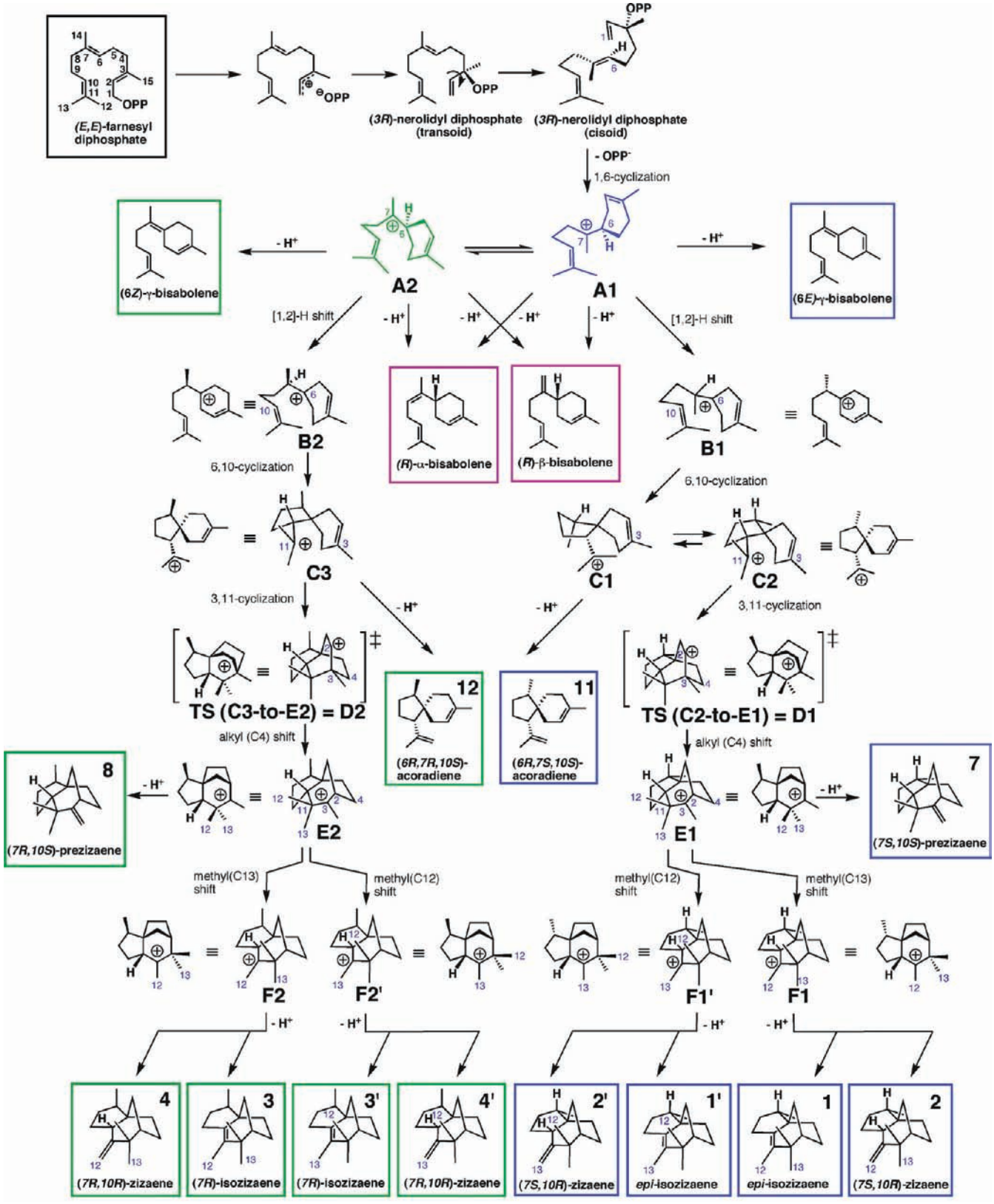

structure for the rearrangement resembles this previously proposed structure. Other concerted mechanisms of this sort, where the formation of a discrete secondary cation is avoided and a tertiary cation is formed directly, have been proposed to account for the C-ring expansion in sterol biosynthesis,[68] cyclopentyl ring formation in trichodiene biosynthesis,[10] cyclosativene and sativene formation,[7] and the formation of abietadiene.[60] In addition, in our preliminary calculations on rearrangements of the terpinyl cation to several monoterpenes, a similar sort of transition structure is observed.[60] Direct deprotonation of **E1** at C15 would generate (7*S*,10*S*)-prezizaene (**7**).

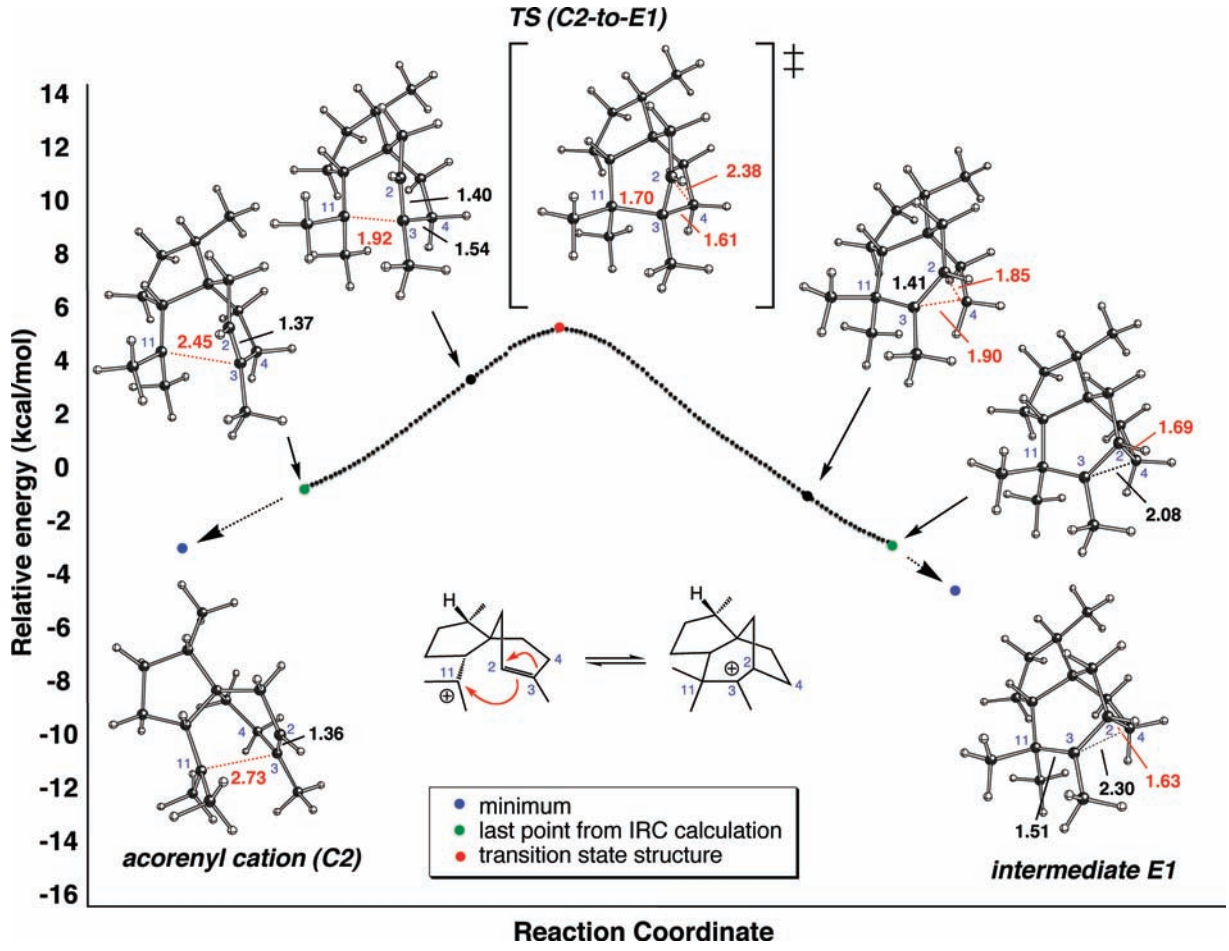

Figure 3. Conversion of acorenyl cation conformer **C2** to **E1** from IRC calculations.

The final step in the *epi*-isozizaene formation mechanism was expected to be the conversion of **E1**-to-**F1** (Scheme 3) via a [1,2]-methyl shift of C13 (based on the originally proposed mechanism by Lin and co-workers).[33] However, neither of the two methyl groups (C12 and C13) on C11 appears to be strongly hyperconjugated with the carbocationic carbon C3, suggesting that there may not be a strong inherent preference for migration of C13. We located two different transition structures that connect **E1** and **F1**, both of which, **TS (E1**-to-**F1)** and **TS′ (E1**-to-**F1)**, again resemble typical bridged nonclassical carbocations, here with penta-coordinated carbons (C13 and C12, respectively; see Figure 2). Our calculations suggest that the C13 methyl shift is less favorable than the C12 methyl shift by ~2 kcal/mol; of course both processes are energetically accessible and this inherent preference could be altered in the enzyme active site.[33] Direct deprotonation of **F1** at C10 would generate *epi*-isozizaene (**1**), while deprotonation from the methyl group on C11 of **F1** would generate (7*S*,10*R*)-zizaene (*epi*-zizaene) (**2**) (see Scheme 3, right).

The transition structure for the conversion of **A1** to **B1** was the highest energy structure in the overall pathway to form *epi*-isozizaene and *epi*-zizaene (Scheme 3, right, and Figure 2). As expected, the energies predicted using B3LYP and mPW1PW91 diverge somewhat as the polycyclization progresses (i.e., as more rings are formed).[58] Nonetheless, both sets of calculations predict that the overall rearrangement from the bisabolyl cation **A1** to cation **E1** is substantially exothermic, as we would expect for a rearrangement in which the number of π-bonds is decreased while the number of σ-bonds is increased. Note also that only one substantial conformational change (**C1**-to-**C2**) was necessary along this pathway. In other words, for most of the pathway, the conformation produced in one step was the productive conformation for the next step.

Formation of (7*R*)-Isozizaene (3), (7*R*,10*R*)-Zizaene (4), (7*R*,10*S*)-Prezizaene (8) and (6*R*,7*R*,10*S*)-Acoradiene (*epi*-*β*-acoradiene) (12). The complete reaction pathway from bisabolyl cation conformer **A2** to (7*R*)-isozizaene (**3**) and (7*R*,10*R*)-zizaene (**4**), based on the results of our quantum chemical calculations, is shown in Scheme 3 (left). The pathway also leads to (7*R*,10*S*)-prezizaene (**8**), (6*R*,7*R*,10*S*)-acoradiene (*β*-acoradiene) (**12**), (6*Z*)-*γ*-bisabolene, and α/*β*-bisabolene, but in contrast to the *epi*-isozizaene (**1**) formation mechanism discussed above, a [1,2]-hydride shift to the pro-*R* face of the cationic center is required to produce the stereoisomer ((7*R*)-**B2**) of the homobisabolyl cation (Scheme 2) that will lead to (7*R*)-isozizaene (**3**) and (7*R*,10*R*)-zizaene (**4**) (Scheme 3). The overall pathway is very similar to the pathway described above that leads to the epimeric *epi*-isozizaene (**1**), (7*S*,10*R*)-zizaene (**2**), (7*S*,10*S*)-prezizaene (**7**), and (6*R*,7*S*,10*S*)-acoradiene (**11**) (see Supporting Information for details). In this case, however, no conformational change of cation **C** is required in preparation for the subsequent cyclization/alkyl shift step.

(68) Hess, J. B. A. *J. Am. Chem. Soc.* **2002**, *124*, 10286–10287.

Scheme 4

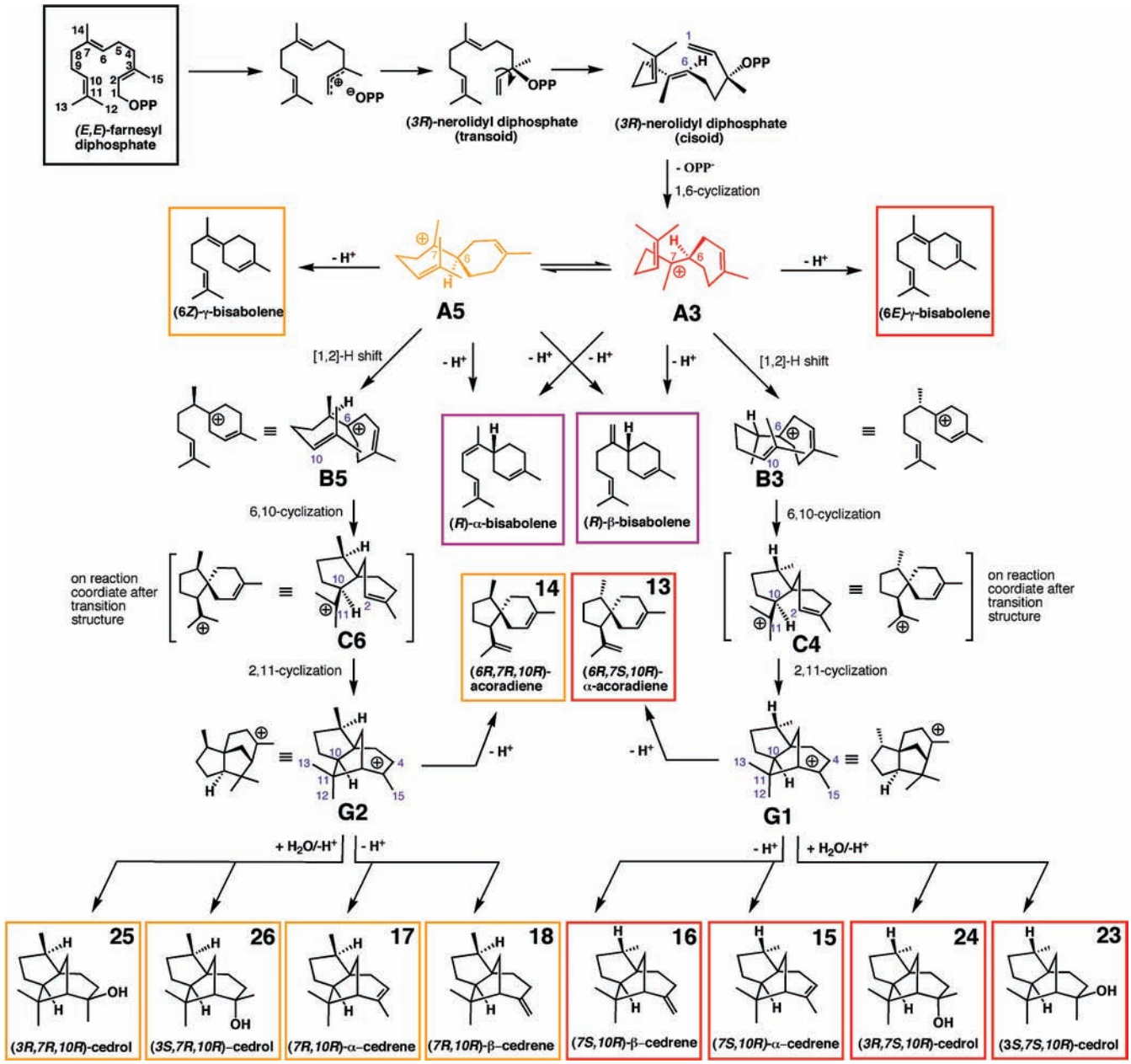

Formation of (7*S*)-α-Cedrene (15), (7*S*)-*β*-Cedrene and (6*R*,7*S*,10*R*)-Acoradiene (α-Acoradiene) (13). The hydrocarbon skeleton of cedrene (Scheme 2) differs from that of zizaene, although both are tricycles containing two 5- and one 6-membered rings. A complete reaction pathway from bisabolyl cation conformer **A3** to the cedrenes **15** and **16** (and the cedrols, **23** and **24**, which are also observed in Nature; Chart 1) is shown in Scheme 4 (right).[16] This pathway also leads to (6*R*,7*S*,10*R*)-acoradiene (α-acoradiene) (**13**), (6*E*)-γ-bisabolene, and α/*β*-bisabolene. Conformer **A3** differs from conformer **A1** (Figure 2) primarily in the orientation of the C10═C11 bond and the cyclohexene ring with respect to the acyclic chain (see Supporting Information for details). Thus, these conformers are interconvertible by rotations about the C9−C10 and C6−C7 bonds.

In the proposed mechanism for cedrene formation (Scheme 2), the first step after the formation of the bisabolyl cation again consists of a [1,2]-hydride shift. This [1,2]-hydride shift (via the "exterior" face of the acyclic chain of **A3**) converts **A3** into the homobisabolyl cation conformer (*7S*)-**B3** (Scheme 4, right) that is productive for the subsequent 6,11-spirocyclization. Attack of the C10═C11 π-bond on carbocation center C6 was expected to convert cation **B3** to the acorenyl cation (**C**, Schemes 2 and 4), with the 10*R* configuration, but surprisingly, we were unable to locate a minimum corresponding to this acorenyl cation. Instead we located a transition structure, **TS** (**B3-to-G1**) (Figure 4) that connects **B3** and cation **G1** directly. Deprotonation of **G1** leads to the (*7S*)-cedrenes **15** and **16** (and capture by water leads to the (*7S*)-cedrols **23** and **24**). The direct conversion of **B3** into **G1** was not only unexpected, but it also distinguishes the cedrene formation mechanism from the zizaene and isozizaene formation mechanisms where acorenyl cations were located (e.g., Figure 2). Direct generation of **G1** again involves a concerted rearrangement with two asynchronous events: 6,10-cyclization and 2,11-cyclization (Figure 4).[67]

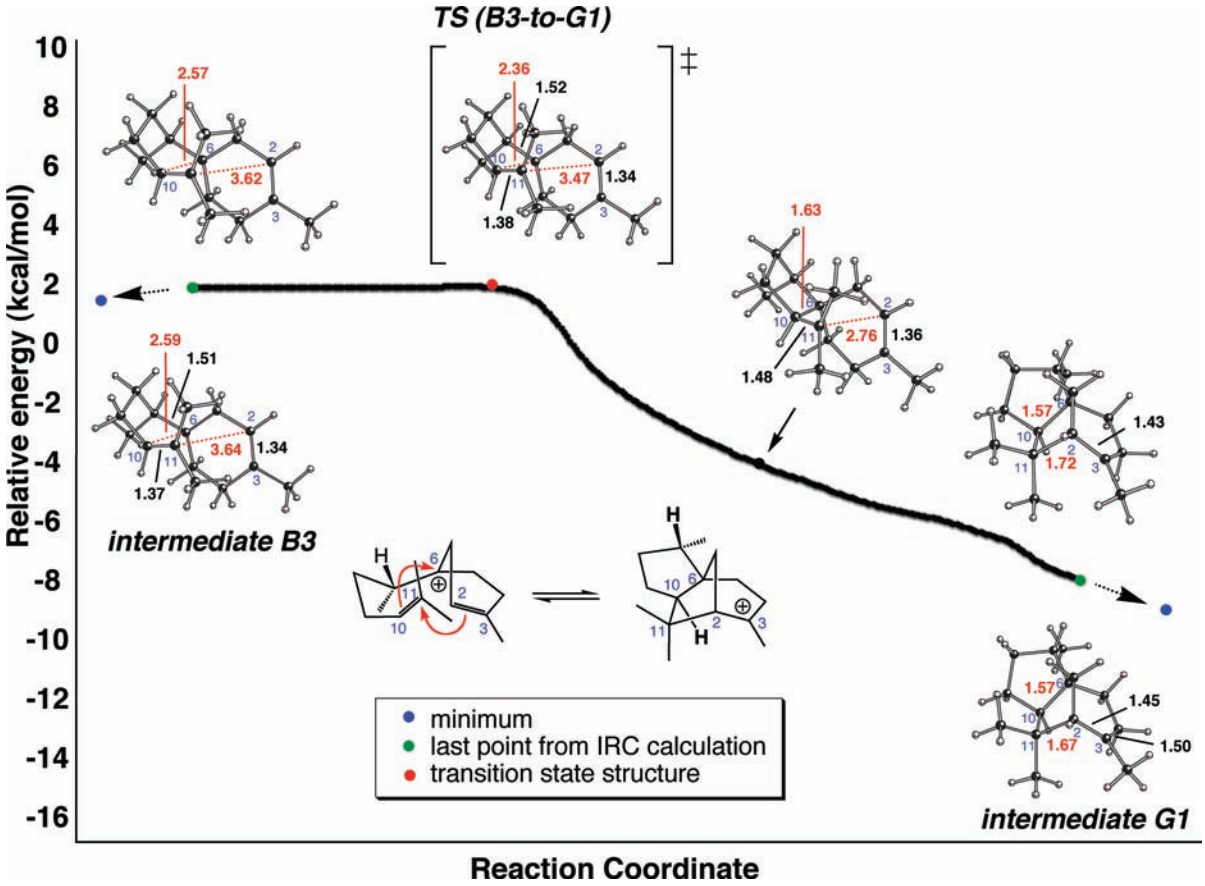

Figure 4. Conversion of homobisabolyl cation conformer **B3** to **G1** from IRC calculations.

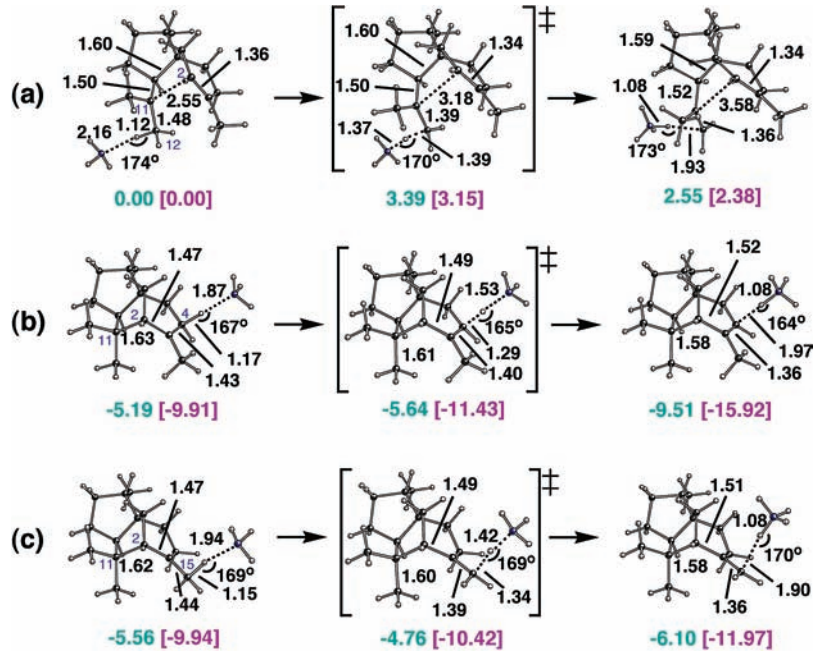

Figure 5. Ammonia−**G1** complexes, transition state structures for deprotonation, and complexes of product alkenes with ammonium. (a−c) show complexation and deprotonation at three different locations. Selected distances are shown in Å. Computed relative energies in kcal/mol (relative to the energy of complex **G1**···NH_3 in (a)) are from B3LYP/6-31+G(d,p)//B3LYP/6-31+G(d,p) and mPW1PW91/6-31+G(d,p)//B3LYP/6-31+G(d,p) calculations, blue and plum in brackets, respectively.

Similar transformations have been described in the context of pentalenene formation[9] and steroid biosynthesis.[66,68] The expected acorenyl cation structure does appear on the reaction coordinate for the **B3**-to-**G1** reaction, but it is not a minimum (see Figure 4). This is presumably a result of the close proximity and appropriate alignment of the cyclohexenyl double bond and the tertiary carbocationic center in such structures. Interestingly, there was essentially no energetic barrier for the conversion of **B3** to **G1**, suggesting that (at least in the absence of the enzyme active site) this process is also effectively (if not technically)

Scheme 5

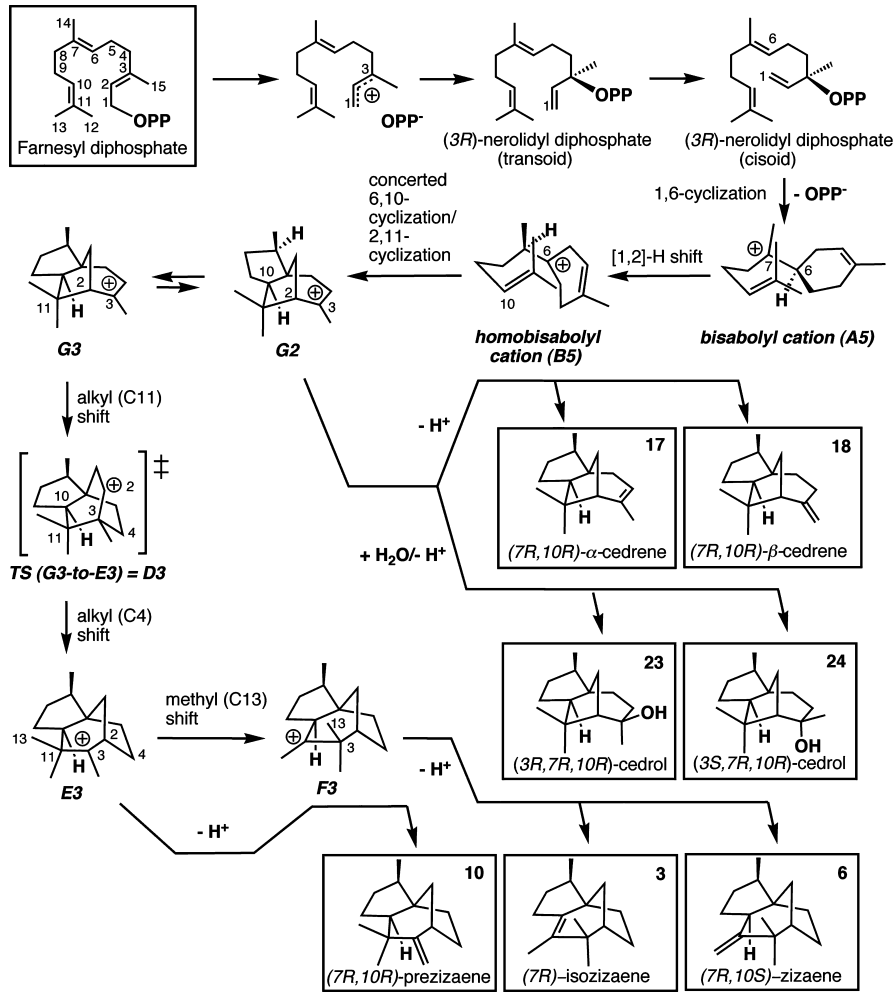

merged with the initial [1,2]-hydrogen shift. This is a striking example of the impact of conformational preorganization.

Direct deprotonation at C4 or C15 of **G1** leads to α-cedrene (**15**) or β-cedrene (**16**) (Scheme 4) Alternatively, (6*R*,7*S*,10*R*)-acoradiene (α-acoradiene) (**13**) could be generated by deprotonation at C12 or C13 of **G1**, coupled with cleavage of the C11−C2 σ-bond. To see if deprotonation at C12, for example, can indeed lead to C11−C2 cleavage, we examined proton transfer from **G1** to ammonia (a simple model base; Figure 5a).[7,53,55] Although it is unlikely that a simple amine will be found in the active site of a sesquiterpene synthase, residues such as histidine have been found in terpene synthase active sites.[69] In the uncomplexed structure of cation **G1**, the C11−C2 σ-bond is elongated (1.67 Å) due to hyperconjugation. This distance is elongated much further (to 2.55 Å) merely upon complexation with ammonia (Figure 5a). Thus, it seems that the interaction of an active site base with a C−H bond of **G1** that is antiperiplanar to the C11−C12 bond would promote a change in the **G1** structure toward that of the previously proposed acorenyl cation intermediate (**C4**), facilitating deprotonation to form acoradiene. We have observed similarly large geometric distortions to carbocation structures upon their participation in intermolecular C−H···X interactions for other systems with appropriately oriented C−H and C−C bonds.[7,53,55] For comparison, C4 and C15 deprotonation are shown in Figure 5b,c. Note that complexation with the hydrogens at these carbons actually slightly decreases the C11−C2 distance, since electron donation from the ammonia lone pair to the cationic center via the intervening C−H bond reduces the ability of that center to participate in hyperconjugation with the C11−C2 bond. These examples hint that appropriately oriented electron rich groups (i.e., C−H···X acceptors) in sesquiterpene synthase active sites may play key roles in determining product distributions by manipulating the structures of intermediate carbocations and the transition structures connected to them.[70]

Formation of (7*R*,10*R*)-α-Cedrene (*epi*-α-cedrene) (17), (7*R*,10*R*)-*β*-Cedrene (*epi*-*β*-Cedrene) (18) and (6*R*,7*R*,10*R*)-Acoradiene (*epi*-α-Acoradiene) (14). The complete reaction pathway from bisabolyl cation conformer **A5** to (7*R*,10*R*)-α-cedrene (*epi*-α-cedrene) (**17**), (7*R*,10*R*)-β-cedrene (*epi*-β-cedrene) (**18**) and the corresponding cedrols (**25** and **26**), based on our calculations is shown in Scheme 4 (left). This pathway also leads to (6R,7*R*,10*R*)-acoradiene (*epi*-α-acoradiene) (**14**), (6*Z*)-γ-bisabolene, and α/β-bisabolene. This pathway is extremely similar to that described above for the formation of cedrene and α-acoradiene (Scheme 4, right; see Supporting Information for details) and therefore will not be discussed further here.

(69) E.g.: Lesburg, C. A.; Zhai, G.; Cane, D. E.; Christianson, D. W. *Science* **1997**, *277*, 1820–1824.

(70) The potential of an alternative conformer of the bisabolyl cation **A4** to undergo similar rearrangements was also examined, and detailed results can be found in the Supporting Information. For this system, we were able to locate an acorenyl cation with the 10*R* configuration (**C5**).

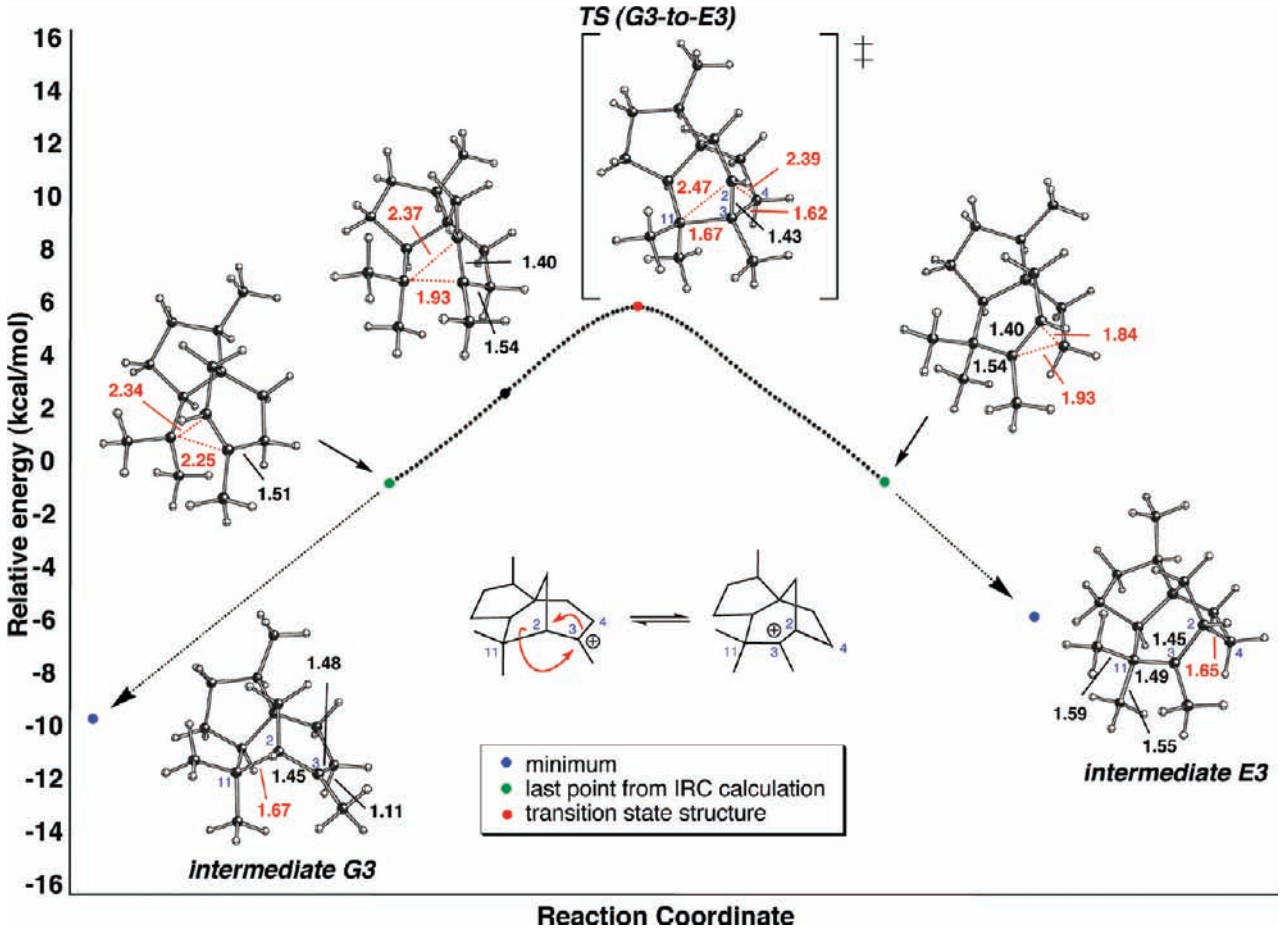

Figure 6. Conversion of **G3** to **E3** from IRC calculations.

Formation of (7*R*)-Isozizaene (3) and (7*R*,10*S*)-Zizaene (10-*epi*-Zizaene) (6) via the Cedrene Pathway. We also explored the possibility of forming (7*R*)-isozizaene (**3**) and (7*R*,10*S*)-zizaene (10-*epi*-zizaene) (**6**) from intermediate **G** on the cedrene pathway (Scheme 2, **G** → **D**), which can be an alternative for the generally proposed mechanism to form prezizaene (Scheme 2, **C** → **D**),[35,39] A reaction pathway based on our calculations is shown in Scheme 5. Consistent with the observations on *epi*-isozizane and zizaene formation described above, we were unable to locate a minimum corresponding to cation **D**. Instead we located a transition structure (**TS (G3**-to-**E3)**, Figure 6), which is very similar to transition structure **TS (C3**-to-**E2)** (**D2**, Scheme 3, left), but differs in its C10 configuration. This is quite interesting in that these two transition structures correspond to rather different rearrangements, since one is connected to an acorenyl cation while the other is connected to a cation of type **G**. The generation of **E3** from **G3** involves a dyotropic rearrangement of **G3** where the two bond shifting events occur quite asynchronously (Figure 6).[67,71−75] Direct deprotonation of **E3** would generate (7*R*,10*R*)-prezizaene (**10**).

In contrast to the *epi*-isozizaene and zizaene formation mechanisms described above, the C13−C11 bond of **E3** appears to be substantially hyperconjugated with the carbocation center C3 (Figure 6). Conversion of **E3** to **F3** via C13 methyl shift has a barrier of ∼4 kcal/mol from **E3**. Direct deprotonation from C12 of **F3** will generate (7*R*)-isozizaene (**3**), however alternative deprotonation from C10 of **F3** will generate (7*R*,10*S*)-zizaene (**6**, Scheme 5), which is an epimer of **4** (Scheme 3). To the best of our knowledge, neither (7*R*,10*R*)-prezizaene (**10**) nor (7*R*,10*S*)-zizaene (**6**) have yet been isolated from natural sources.[35] In a recent study on tobacco 5-*epi*-aristolochene synthase, however, O'Maille and co-workers reported coisolation of (7*S*,10*R*)-α-cedrene (**15**), (7*S*,10*R*)-α-acoradiene (**13**), and (7*S*,10*R*)-prezizaene (**9**).[39]

Formation of (7*R*,10*S*)-Cedrenes (21 and 22), (7*R*,10*S*)-Duprezianenes (37 and 38), and Sesquithuriferols (33 and 34). 2,11-Cyclization of the (7*R*,10*S*)-acorenyl cation (**C3**, Scheme 3) is expected to lead to cation (7*R*,10*S*)-**G4** (Schemes 2 and 6). Direct deprotonation (7*R*,10*S*)-**G4** would generate (7*R*,10*S*)-α/β-cedrene (**21** and **22**).[76] Alternatively, an alkyl shift could convert (7*R*,10*S*)-**G4** to secondary cation **H** (Schemes 2 and 6). While water capture by **H** could generate sesquithuriferols **33** and **34**, a subsequent alkyl shift could lead to **I**, the precursor of the duprezianenes.[37,38]

We located a transition structure connecting acorenyl cation conformer **C3** to cation **G4** (Figure 7). The 2,11-cyclization of **C3** occurs with only a small energy barrier (Figure 8) and both B3LYP and mPW1PW91 calculations indicate that this conver-

(71) Nouri, D. H.; Tantillo, D. J. *J. Org. Chem.* **2006**, *71*, 3686–3695.
(72) Reetz, M. T. *Angew. Chem., Int. Ed. Engl.* **1972**, *11*, 130–131.
(73) Reetz, M. T. *Angew. Chem., Int. Ed. Engl.* **1972**, *11*, 129–130.
(74) Reetz, M. T. *Tetrahedron* **1973**, *29*, 2189–2194.
(75) Reetz, M. T. *Adv. Organomet. Chem.* **1977**, *16*, 33–65.

(76) We have also explored the formation of (7*R*,10*S*)-cedrenes (**21** and **22**) in the presence of a base. See Supporting Information for details.

Scheme 6

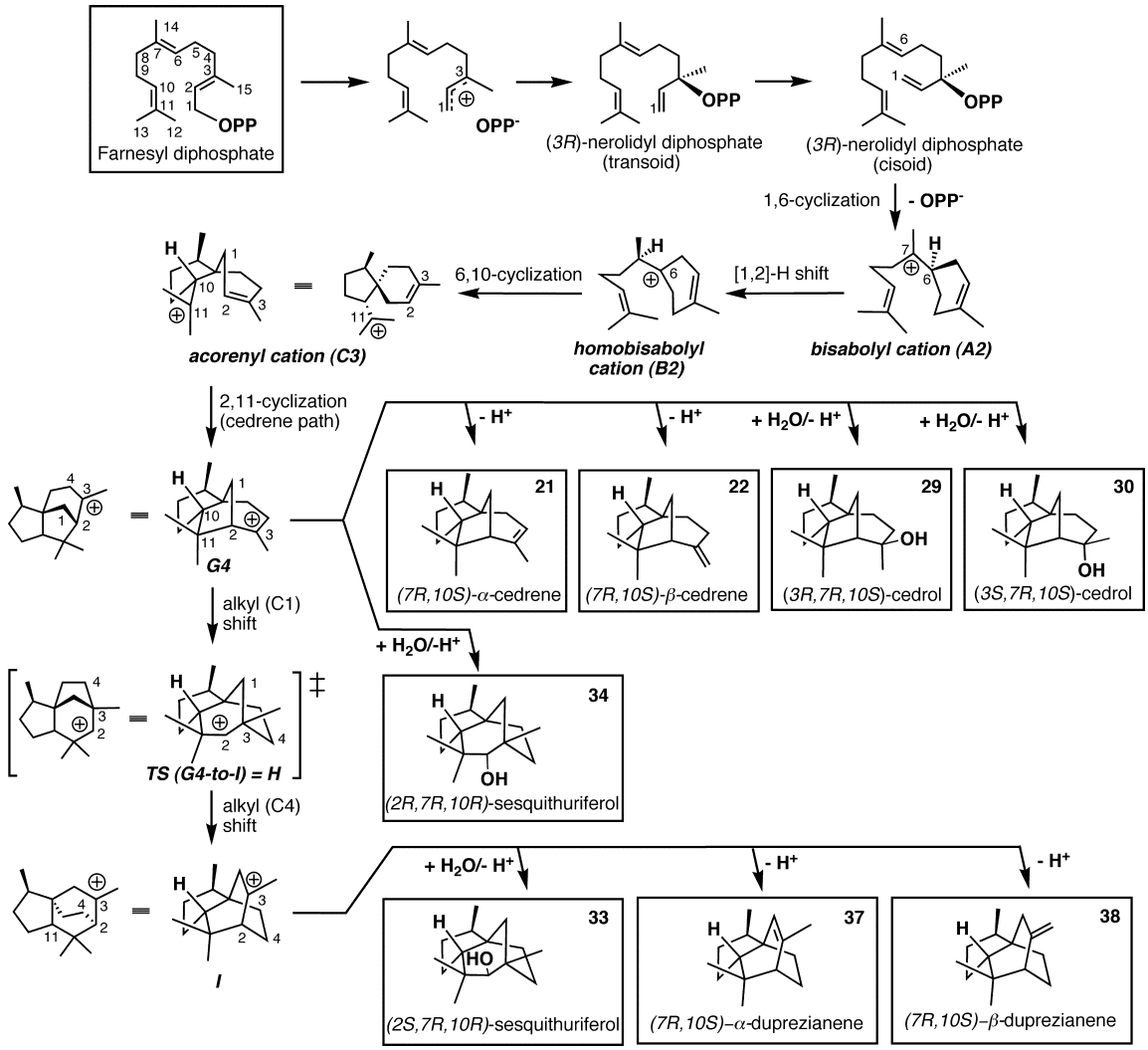

sion is an endothermic process (by ~1−5 kcal/mol). In the structure of **G4**, the C1−C2 σ-bond (1.67 Å) is hyperconjuated with cationic center C3, which differs from the sort of hyperconjugation observed for the alternative conformers **G1** and **G2**, which have elongated C11−C2 σ-bonds (1.67 Å and 1.68 Å, respectively; see Supporting Information). As described above (see Scheme 3), acorenyl cation conformer **C3** can also be converted to cation **E2**. As shown in Figure 8, this process (3,11-cyclization) is kinetically disfavored with respect to **G4** formation (2,11-cyclization), although it is thermodynamically favored.

The next step in the proposed rearrangement is the conversion of **G4** to **H** (Schemes 2 and 6). We located a structure that resembles the hypothetical secondary cation **H**; however, it is not a minimum but is instead a transition structure connecting **G4** directly to **I** (Figure 7). This conversion is another concerted but asynchronous dyotropic rearrangement.[67,71–75] Direct deprotonation of **I** would lead to (7*R*,10*S*)-α/β-duprezianene (**37**/**38**).[37,38]

Sesquithuriferol is expected to be derived from hypothetical secondary cation **H** by water capture (Scheme 2), but, as mentioned above, we were not able to locate such a secondary cation as a minimum in the gas phase. Nevertheless, we were able to locate a transition structure that resembles the expected transition structure for water addition to **H** (Figure 9). This transition structure actually connects an ion−molecule complex of cation **I** with water to protonated sesquithuriferol (Scheme 7a and Figure 9). In the **I**·H_2O complex, the water molecule interacts with C15−H via a C−H···X interaction (Figure 9).[53,55] Based on IRC calculations (see Figure 9), attack of H_2O occurs at C2 of **I** and is accompanied by an alkyl (C4) shift from C2 to C3. Note that in the transition structure, the partial C2---O bond is antiperiplanar to the C3−C4 bond. This process generates (2*S*,7*R*,10*R*)-sesquithuriferol (**33**, after deprotonation). Interestingly, conversion of (2*S*,7*R*,10*R*)-sesquithuriferol (**33**) to α/β-duprezianenes upon treatment with tosyl chloride/pyridine has been reported by Barrero and co-workers, whose proposed mechanism also involves a concerted tosyl group departure and alkyl shift.[37,38]

We also located a transition structure that appears to correspond to water addition to the other face of the hypothetical carbocation **H** to form (2*R*,7*R*,10*R*)-sesquithuriferol (**34**). This transition structure does connect an ion−molecule complex of cation **H**, which does not exist as a minimum in the absence of H_2O, with water and protonated sesquithuriferol (Scheme 7b). In this **H**·H_2O complex the water molecule directly interacts with the empty p-orbital of C2 (at a C2---O distance of 2.63 Å; see Supporting Information for details). Thus, our calculations suggest that the nature of cation **H** depends on the nature of the environment in which it is formed.

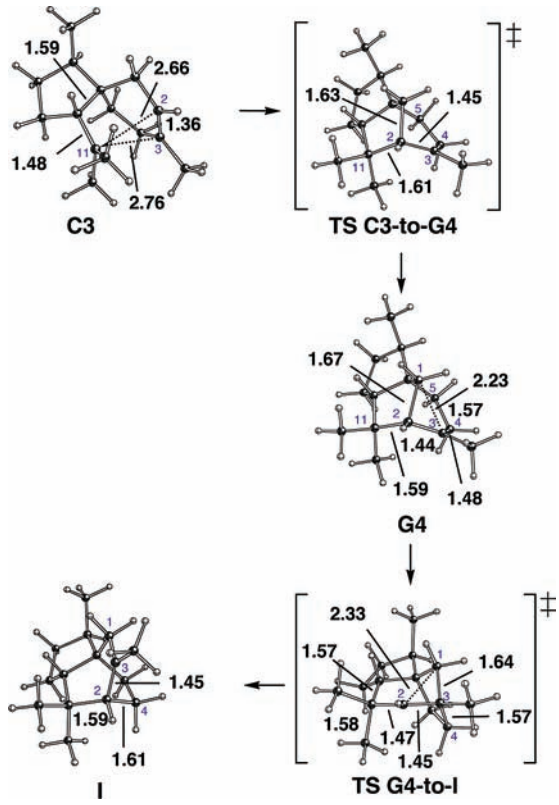

Figure 7. Computed geometries (B3LYP/6-31+G(d,p)) for stationary points involved in the conversion of **C3** to **I**. Selected distances are shown in Å.

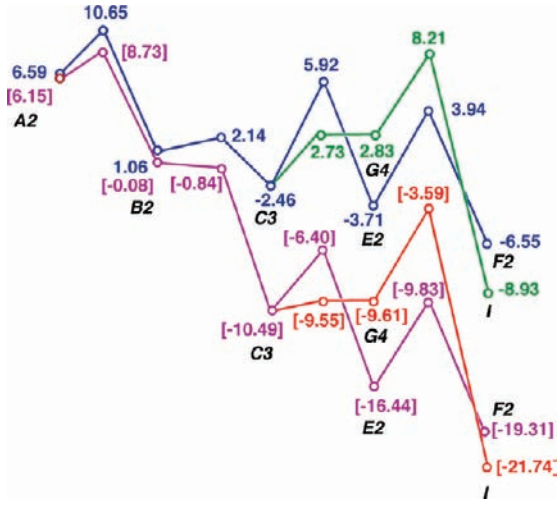

Figure 8. Energetics for formation of **F2** and **I**. Blue and green: B3LYP/6-31+G(d,p)//B3LYP/6-31+G(d,p). Plum and red in brackets: PW1PW91/6-31+G(d,p)//B3LYP/6-31+G(d,p).

4. Implications

4.1. Substrate Preorganization. Given the key role of the bisabolyl cation in the pathways to the bisabolene, curcumene, zizaene, cedrene, acoradiene, duprezianene, and sesquithuriferol sesquiterpenes, among others (see Scheme 1), it is important to understand the relationship between bisabolyl cation conformers and the ultimate sesquiterpene products to which they are directly connected. Herein we describe four conformers of the bisabolyl cation, **A1**, **A2**, **A3**, and **A5**, which differ in the orientation of their acyclic hydrocarbon chains. Figure 10 shows which of these conformers leads directly to which sesquiterpene products. Given that known sesquiterpene synthases utilize exclusively (*E*,*E*)-FPP, these conformers of the bisabolyl cation fall into two forms: those that are productive and accessible from direct cyclization of FPP/NPP (**A1** and **A3**) and those that are productive but cannot be formed directly from FPP/NPP (**A2** and **A5**). We suggest then that conformational changes from accessible to initially inaccessible bisabolyl cation conformers are necessary in order to form zizaene and *epi*-cedrene, for example. In other words, FPP cannot be preorganized to form the conformers of the bisabolyl cation that lead directly to certain sesquiterpenes, since one of its C=C double bonds would have to have a *Z* configuration. It is unclear at this point if such conformational interconversions might be connected to protein conformational changes occurring upon pyrophosphate departure.[19,21,77] If this model is correct, then the productive conformation of the bisabolyl cation does not necessarily reflect the original orientation of farnesyl diphosphate bound in the corresponding enzyme active site. This implies then that the shape of the active site for some of the cases we describe herein might be preorganized for binding to *the productive bisabolyl cation conformer* rather than an accessible conformer of FPP.

4.2. Absolute Configuration of the Bisabolyl Cation. In general, the co-occurrence of sesquiterpene (or sesquiterpenoid) stereoisomers that differ in configuration at C6 or C7 is sometimes explained by invoking the intermediacy of both *R* and *S* bisabolyl cation intermediates, either in two different enzymes or in the same enzyme.[15,29,36,78] On the basis of our results, we suggest an alternative. We find it unlikely that conformations of farnesyl diphosphate (and subsequently nerolidyl diphosphate) that can lead to both enantiomers of the bisabolyl cation would be accommodated and bound sufficiently tightly in most sesquiterpene active sites (although this may be possible for some of the more promiscuous sesquiterpene synthases).[79] Instead, we suggest that binding to one conformer of NPP to produce one or the other (*R* or *S*) bisabolyl cation stereoisomer can lead to products that appear to have arisen from both. This is possible because conformational adjustment of the acyclic portion of the bisabolyl cation can occur before the [1,2]-hydrogen shift that forms the homobisabolyl cation, an intermediate in all the pathways described herein (see Schemes 3 and 4). This conformational adjustment allows both C7-epimers of the homobisabolyl cation to be formed from the *same* bisabolyl cation stereoisomer. A similar contention has been put forth in the context of the promiscuous TPS4 synthase from maize, for which homology modeling and docking studies have suggested that two different conformers of the bisabolyl cation may bind to the active site in different pockets.[20,29] On the basis of these results, the authors suggested that these conformers can interconvert during the reaction and produce epimeric products. Interestingly, the detection of only one

(77) Vedula and coworkers observed that metal−pyrophosphate coordination is disturbed upon carbocation binding with tricodiene synthase. See: Vedula, L. S.; Zhao, Y.; Coates, R. M.; Koyama, T.; Cane, D. E.; Christianson, D. W. *Arch. Biochem. Biophys.* **2007**, *466*, 260–266. See also ref 78.
(78) Vedula, L. S.; Jiang, J.; Zakharian, T.; Cane, D. E.; Christianson, D. W. *Arch. Biochem. Biophys.* **2008**, *469*, 184–194.
(79) Steele, C. L.; Crock, J.; Bohlmann, J.; Croteau, R. *J. Biol. Chem.* **1998**, *273*, 2078–2089.
(80) Carpenter, B. K. *Annu. Rev. Phys. Chem.* **2005**, *56*, 57–89.

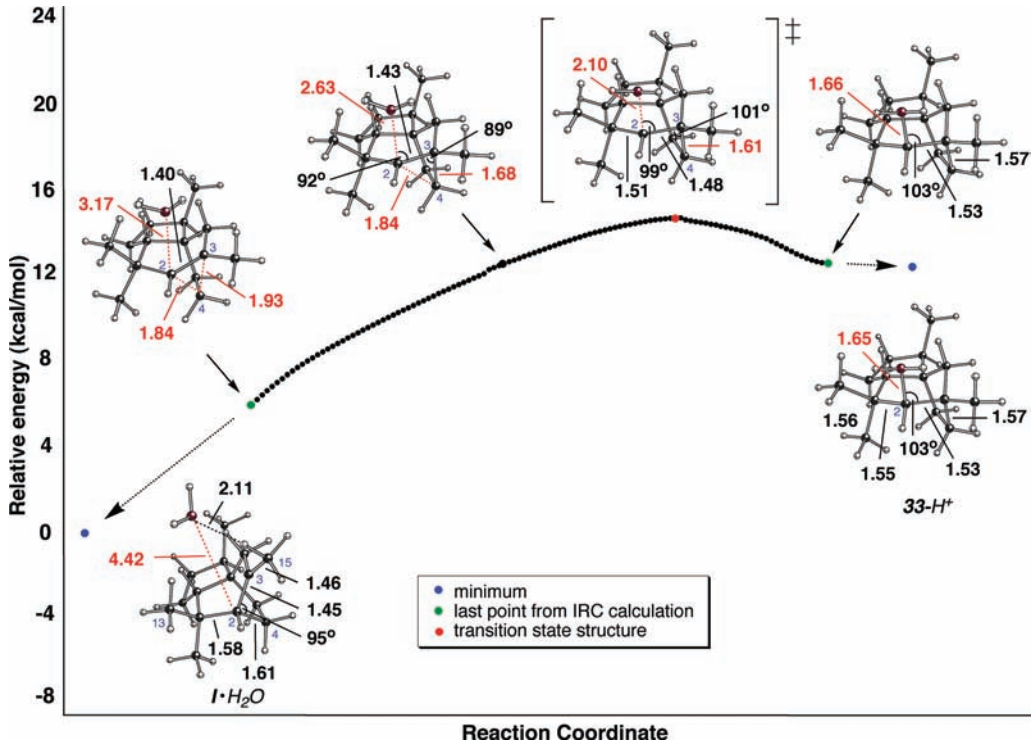

Figure 9. Conversion of **I**·H_2O to **33**−H^+ from IRC calculations.

Scheme 7

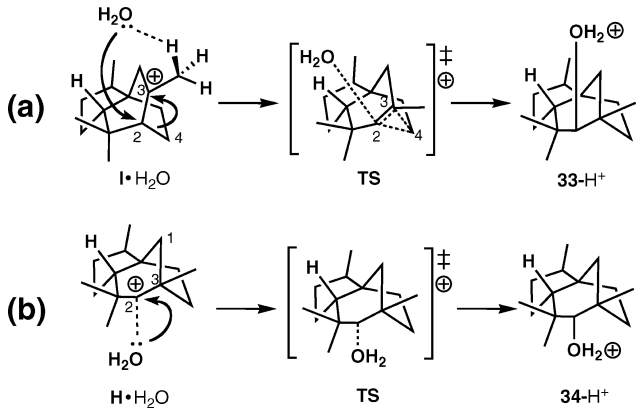

epimer of β-bisabolene has been reported as a product in this system, consistent with all of the stereoisomeric products being derived from the (*S*)-bisabolyl cation. Similar scenarios may also be relevant to cedrene and *epi*-cedrene formation from *Osyris tenuifolia*,[36] (*E*)- and (*Z*)-bergamotene formation from *Osyris tenuifolia*,[36] α- and β-acoradiene formation by the trichodiene synthase mutant from *Fusarium sporotrichioides*,[78] and β-santalene and *epi*-β-santalene formation from *Santalum album*.[15]

4.3. Secondary Carbocations. Based on our results, many of the previously proposed mechanisms for the production of the sesquiterpenes desribed herein are plausible and energetically favorable, but we suggest that several of these be modified in subtle but important ways. The main difference between the previous proposals and our suggested variants is that we were unable to locate any of the secondary carbocations that had been proposed as intermediates in the sesquiterpene forming reactions described herein as true minima (in the absence of an enzyme). Such structures were instead readily avoided, and concerted rearrangements with asynchronously occurring events were found in their place.[67] Whether or not the avoidance of secondary cations and the presence of such rearrangements will be a general theme in terpene biosynthesis remains to be seen. We have encountered other systems where secondary cations appear to be avoided,[7,10,60,67] but we have also located secondary cations (albeit highly hyperconjugated) as minima in reactions that lead to the sesquiterpene pentalenene[9] and the diterpene abietadiene.[60] In addition, most of the calculations described herein do not yet take into account the effects of a surrounding enzyme active site. In the cases where we have included models of active site residues in our calculations, here and previously,[7,53,55] we have found evidence that the geometries of some cations can be changed significantly when such residues are present. Of particular note are our calculations on (6*R*,7*S*,10*R*)-α-acoradiene (**13**, Figure 5) and sesquithuriferol (**33**, Figure 9) formation where we were able to locate complexes of secondary cations as a minima. Thus, we consider the contention that most secondary cations are avoided in biology to be a tentative hypothesis at this time, but one that is plausible and intriguing enough to pursue further, in no small part because the avoidance of particular intermediates allows the system in question to also avoid byproducts that might arise from them.

4.4. Preorganization of Intermediates. The absence of secondary cations in these mechanisms in a sense streamlines these processes in that fewer intermediates are involved. Another sort of streamlining that we observed is connected to conformational preorganization of the structures involved in any given pathway. In almost every case described above, the product of one step of a given rearrangement is formed, inherently, in a conformation that is productive for the next step of the rearrangement. While conformational changes of some intermediates might be feasible (if a given sesquiterpene

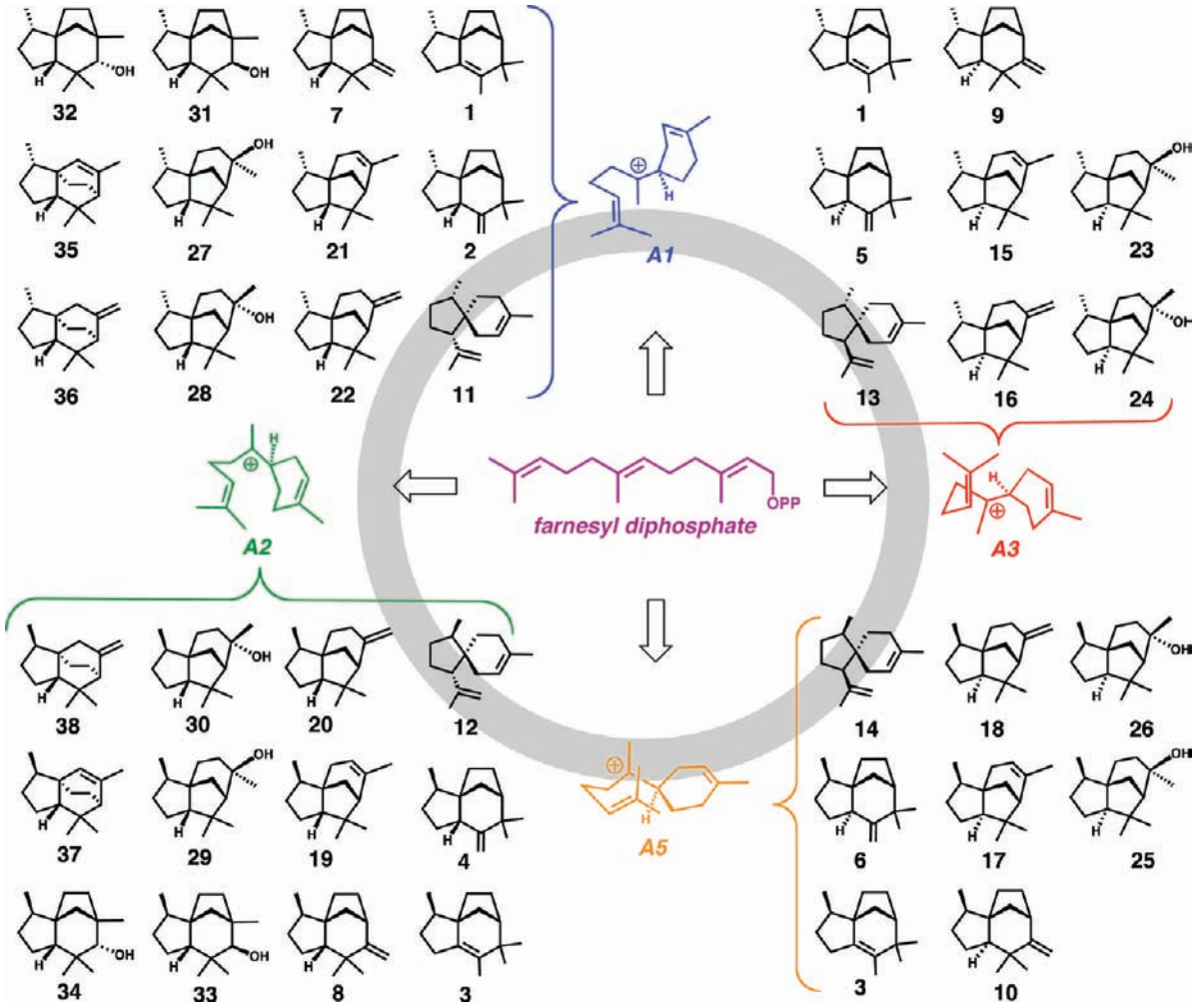

Figure 10. Bisabolyl cation conformers and sesquiterpene products formed from them.

synthase active site is spacious enough or flexible enough),[7] so-called "dynamic matching"[80] may well discourage such conformational changes. In other words, once a system heads down a particular pathway, it will be more likely to get to the end of this pathway rather than diverting onto another pathway via a conformational change. This seems all the more likely given that the barriers for most of the rearrangement steps we describe herein are low and most of these steps are exothermic (in many cases the result of trading π-bonds for σ-bonds).

4.5. C−H···X Interactions. We described herein several cases of intermolecularly modulated intramolecular stereoelectronic effects (e.g., see Figure 5). These are cases where C−H···X interactions between electron rich groups surrounding a carbocation and particular C−H bonds of the cation lead to significant changes to the cation geometry.[7,53,55] The implication of this for enzyme-promoted carbocation rearrangements is clear: appropriately oriented noncovalent interactions can affect the nature of species involved in the rearrangement, potentially biasing reactivity such that particular pathways are followed. It is important to emphasize that for such interactions to have a significant effect, the orientation of the groups involved must be rigidly controlled. For example, as shown above, interacting with some of the hydrogens on a cation but not others (even on the same carbon) leads to a significant geometric change. This is the result of these particular C−H bonds being aligned, for example, with the (formally) vacant p-orbital of a cationic center. Although we have used ammonia as a simple model of a C−H···X acceptor here, this role is likely to be played by residues like histidine, peptide carbonyl groups, bound water, or bound pyrophosphate in the actual biological systems. Efforts to model carbocation complexes with such groups are ongoing.

5. Conclusions

The results of our calculations lead us to conclude that: (1) Correct folding of farnesyl diphosphate alone does not always dictate the structure of cyclization products. (2) Secondary carbocations are often avoided as intermediates in sesquiterpene-forming carbocation rearrangements. (3) Most of the rearrangements described herein do not involve significant conformational changes for the intermediates produced. This, by way of "dynamic matching", may contribute significantly to product selectivity. Note that here we are shifting focus from the conformation of bound FPP to the productive conformation of the bisabolyl cation. (4) C−H···X interactions between electron-rich groups in a sesquiterpene synthase active site can alter the structure of cationic intermediates and transition structures, but only if these groups are oriented properly.

The theoretical approaches described herein are amenable to analyzing a wide variety of terpene synthases.[45] Such efforts, including expanding our calculations to include larger portions of terpene synthase active sites, are ongoing. Overall, we hope that our findings will be useful to both theoreticians and experimentalists interested in understanding the structure−function relationships of terpene synthases.

Acknowledgment. We gratefully acknowledge UC Davis, the National Science Foundation's CAREER program, and the National Science Foundation's Partnership for Advanced Computational Infrastructure (Pittsburgh Supercomputer Center) for support. We thank Mike Lodewyk for helpful comments.

Supporting Information Available: Coordinates and energies for all computed structures, along with the full Gaussian citation (ref 46). This material is available free of charge via the Internet at http://pubs.acs.org.

JA9005332